Theory of Nonlinear Optical Responses in Metal-Dielectric Composites

Andrey K. Sarychev[1,2] and Vladimir M. Shalaev[3]

[1] Center for Applied Problems of Electrodynamics, Moscow, 127412, Russia
[2] Department of Physics, New Mexico State University, Las Cruces, NM 88003, USA
[3] School of Electrical and Computer Engineering, Purdue University, West Lafayette, IN 47907-1285, USA
shalaev@purdue.edu

Abstract. In random metal–dielectric composites near the percolation threshold, surface plasmons are localized in small nanometer-sized areas, hot spots, where the local field can exceed the applied field by several orders of magnitude. The high local fields result in dramatic enhancement of optical responses, especially, nonlinear ones. The local-field distributions and enhanced optical nonlinearities are described using scale renormalization. A theory predicts that the local fields consist of spatially separated clusters of sharp peaks representing localized surface plasmons. Experimental observations are in good accord with theoretical predictions. The localization of plasmons maps the Anderson localization problem described by the random Hamiltonian with both on- and off-diagonal disorder. The feasibility of nonlinear surface-enhanced spectroscopy of single molecules and nanocrystals on percolation films is shown.

1 Introduction

Metal–dielectric composites attract much attention because of their unique optical properties, which are significantly different from those of constituents forming the composite [1,2,3]. Semicontinuous metal films can be produced by thermal evaporation or sputtering of metal onto an insulating substrate. In the growing process, first, small metallic grains are formed on the substrate. The typical size a of a metal grain is about 5 to 50 nm. As the film grows, the metal filling factor increases, and coalescence occurs, so that irregularly shaped self-similar clusters (fractals) are formed on the substrate. The concept of scale-invariance (fractality) plays an important role in the description of various properties of percolation systems [2,4]. The sizes of the fractal structures diverge in the vicinity of the percolation threshold, where an "infinite" percolation cluster of metal is eventually formed, representing a continuous conducting path between the ends of a sample. At the percolation threshold, the metal–insulator transition occurs in the system. At higher surface coverage, the film is mostly metallic, with voids of irregular shape. With further coverage increase, the film becomes uniform.

V. M. Shalaev (Ed.): Optical Properties of Nanostructured Random Media, Topics Appl. Phys. **82**, 169–184 (2002)

In random metal–dielectric films, surface plasmon excitations are localized in small nanometer-scale areas referred to as "hot spots" [2,5,6]. As discussed below, the localization can be attributed to the Anderson localization of plasmons in semicontinuous metal films near a percolation threshold (in this case, referred to as percolation films). Electromagnetic energy is accumulated in the hot spots associated with localized plasmons, leading to local fields that can exceed the intensity of the applied field by four to five orders of magnitude. The high local fields in the hot spots also result in dramatically enhanced *nonlinear* optical responses proportional to the local field raised to a power greater than one.

Local electromagnetic field fluctuations and related enhancement of nonlinear optical phenomena in metal–dielectric composites near percolation threshold (percolation composites) have recently become an area of active studies because of many fundamental problems involved and high potential for various applications. Percolation systems are very sensitive to the external electrical field since their transport and optical properties are determined by a rather sparse network of conducting channels and the field concentrates in the "weak" points of the channels. Therefore, composite materials can have much larger nonlinear susceptibilities at zero and finite frequencies than those of its constituents. The distinguished feature of percolation composites, to amplify nonlinearities of its components, was recognized very early [7,8,9,10,11,12], and nonlinear conductivities and susceptibilities have been intensively studied during the last decade (see, for example, [1,13,14,15,16,17]).

Here, we consider relatively weak nonlinearities when the conductivity $\sigma(E)$ can be expanded in a power series of the applied electrical field E and the leading term, i.e., the linear conductivity $\sigma^{(1)}$, is much larger than others. This is typical for various nonlinearities in the optical and infrared spectral ranges considered here. Even weak nonlinearities lead to qualitatively new physical effects. For example, generation of higher harmonics can be much enhanced in percolation composites, and bistable behavior of the effective conductivity can occur when the conductivity switches between two stable values, etc. [18]. We note that the "languages" of nonlinear currents/conductivities and nonlinear polarizations/susceptibilities (or dielectric constants) are completely equivalent, and they will be used here interchangeably.

Local-field fluctuations can be strongly enhanced in the optical and infrared spectral ranges for a composite material containing metal particles that are characterized by a dielectric constant with negative real and small imaginary parts. Then, the enhancement is due to the surface plasmon resonance in metallic granules and their clusters [1,14,19,20]. The strong fluctuations of the local electrical field lead to the enhancement of various nonlinear effects. Nonlinear percolation composites are potentially of great practical importance [21] as media with intensity-dependent dielectric functions and, in particular, as nonlinear filters and optical bistable elements. The optical response of nonlinear composites can be tuned by controlling the volume fraction and morphology of the constituents.

The theory of nonlinear optical processes in metal–dielectric composites is based on the fact that the problem of optical excitations in percolation composites mathematically maps the Anderson transition problem. This allowed us to predict the localization of plasmon excitations in percolation metal–dielectric composites and describe in detail the localization pattern. In areas where the resonant plasmons are localized, "hot spots," a high concentration of electromagnetic energy results in very large local fields and dramatic enhancement of optical responses. We show that the plasmon eigenstates are localized on a scale much smaller than the wavelength of the incident light. Plasmon eigenstates with eigenvalues close to zero (resonant modes) are excited most efficiently by an external field. Since the eigenstates are localized and only a small portion of them are excited by the incident beam, the overlapping of the eigenstates can typically be neglected, that significantly simplifies theoretical consideration, and allows one to obtain relatively simple expressions for enhancements of linear and nonlinear optical responses. It is important to stress again that the plasmon localization length is much smaller than the light wavelength; in that sense, the predicted subwavelength localization of plasmons differs quite from the well-known localization of light due to strong scattering in a random homogeneous medium [23].

We also note that a developed scaling theory of optical nonlinearities in percolation composites opens new means to study the classical Anderson problem, taking advantage of the unique characteristics of laser radiation, namely, its coherence and high intensity.

In spite of major efforts, most of the theoretical considerations of local optical fields in percolation composites are restricted to mean-field theories and computer simulations (for references, see [15,16,17]). The effective medium theory [24] that has the virtue of relative mathematical and conceptual simplicity was extended for the nonlinear response of percolating composites [1,13,25,26,27,28,29,30,31] and fractal clusters [28]. For linear problems, predictions of the effective medium theory are usually sensible physically and offer quick insight into problems that are difficult to attack by other means [1]. The effective medium theory, however, has disadvantages typical of all mean-field theories, namely, it diminishes the role of fluctuations in a system. In this approach, it is assumed that local electrical fields are the same in the volume occupied by each component of a composite. For example, the effective medium theory predicts that the local electrical field should be the same in all metal grains regardless of their local arrangement in a metal–dielectric composite. Therefore, the local field is predicted to be almost uniform, in particular, in metal–dielectric composites near percolation. This is, of course, counterintuitive since percolation represents a phase transition, where according to the basic principles, fluctuations play a crucial role and determine a system's physical properties. Moreover, in the optical spectral range, the fluctuations are anticipated to be dramatically enhanced because of the resonance with the sp modes of a composite.

We developed a rather effective numerical method [32] and performed comprehensive simulations of the local-field distribution and various nonlinear effects in two-dimensional percolation composites - that were random metal–dielectric films [15,33,34,35]. The effective medium approach fails to explain the results of the computer simulations performed. It appears that electrical fields in such films consist of strongly localized sharp peaks resulting in very inhomogeneous spatial distributions of the local fields. In peaks ("hot" spots), the local fields exceed the applied field by several orders of magnitudes. These peaks are localized in nanometer-size areas and can be associated with the sp modes of metal clusters in a semicontinuous metal film. The peak distribution is not random but appears to be spatially correlated and organized in some chains. The length of the chains and the average distance between them increase toward the infrared part of the spectrum.

Nonlinear optical effects depend not only on the magnitude of the field but also on its *phase*, so that a nonlinear signal, in general, is proportional to $\langle |E(\mathbf{r})|^k E^m(\mathbf{r})\rangle$. In this contribution we describe a scaling theory for enhancement of *arbitrary* nonlinear optical process (for both $2d$ and $3d$ percolation composites) and show that enhancement differs significantly for nonlinear optical processes that include photon subtraction (annihilation) and for those that do not. Photon subtraction implies that the corresponding field amplitude in the expression for nonlinear polarization (current) $P^{(n)}$ is complex conjugated [22]. For example, the optical process known as coherent anti-Stokes Raman scattering is driven by the nonlinear polarization $P^{(3)} \propto E^2(\omega_1)E^*(\omega_2)$ which results in generation of a wave at the frequency $\omega_g = 2\omega_1 - \omega_2$, i.e., in one elementary act of this process, the ω_2 photon is subtracted (annihilated); the corresponding amplitude $E(\omega_2)$ in the expression for $P^{(3)}$ is complex conjugated.

In this review, we develop a simple scaling approach explaining extremely inhomogeneous field distribution and giant optical nonlinearities of metal–dielectric composites for an arbitrary optical process. We also show the great potential of percolation films for surface-enhanced local spectroscopy of single molecules and nanocrystals.

2 Percolation and Anderson Transition Problem

We consider here the general case of a three-dimensional random composite. As mentioned, the typical size a of the metal grains in percolation nanocomposites is of the order of 10 nm, i.e., much smaller than the wavelength λ in the visible and infrared spectral ranges, so that we can introduce a potential $\phi(\mathbf{r})$ for the local electrical field. The field distribution problem reduces to the solution of the equation representing the current conservation law:

$$\nabla \cdot \left\{\sigma(\mathbf{r}) \left[-\nabla\phi(\mathbf{r}) + \mathbf{E}^{(0)}(\mathbf{r})\right]\right\} = 0\,, \tag{1}$$

where $\mathbf{E}^{(0)} \equiv \mathbf{E}_0$ is the applied field and $\sigma(\mathbf{r})$ is the local conductivity that takes σ_{m} and σ_{d} values for the metal and dielectric, respectively. In the discretized form, this relation acquires the form of Kirchhoff's equations defined, for example, on a cubic lattice [1].

We can write Kirchhoff's equations in terms of the local dielectric constant $\epsilon = (4\pi \mathrm{i}/\omega)\sigma$, rather than conductivity σ. We assume that the external electrical field $\mathbf{E}^{(0)}$ is directed, say, along the z axis. Thus, in the discretized form, (1) is equivalent to the following set of equations:

$$\sum_j \epsilon_{ij}\left(\phi_i - \phi_j + E_{ij}\right) = 0, \tag{2}$$

where ϕ_i and ϕ_j are the electrical potentials determined at the sites of the cubic lattice (or the square lattice, for a two-dimensional system); the summation is over the six nearest neighbors of the site i. The electromotive force E_{ij} takes the value $E^{(0)}a_0$ for the bond $\langle ij\rangle$ aligned in the positive z direction, where a_0 is the spatial period of the cubic lattice (which can coincide with the size grain a). For the bond $\langle ij\rangle$ aligned in the $-z$ direction, the electromotive force E_{ij} takes the value $-E^{(0)}a_0$; for the other four bonds related to site i, $E_{kj} = 0$. The permittivities ϵ_{ij} take values ϵ_{m} and ϵ_{d}, with probabilities p and $1-p$, respectively. Thus a percolation composite is modeled by a random network, including the electromotive forces E_{ij} that represent the external field.

For simplicity, we can assume that the cubic lattice has a very large but finite number of sites N and rewrite (2) in the matrix form with the "interaction matrix" $\widehat{\boldsymbol{H}}$ defined in terms of the local dielectric constants:

$$\widehat{\boldsymbol{H}}\,\Phi = \mathcal{E}\,, \tag{3}$$

where Φ is the vector of the local potentials $\Phi = \{\phi_1, \phi_2, \ldots, \phi_N\}$ determined at N sites of the lattice. Vector $\mathcal{E}$ also has N components $\mathcal{E}_i = \sum_j \epsilon_{ij}E_{ij}$, as follows from (2). The $N \times N$ matrix $\widehat{\mathrm{H}}$ has off-diagonal elements $H_{ij} = -\epsilon_{ij}$ and diagonal elements $H_{ii} = \sum_j \epsilon_{ij}$ (j refers to the nearest neighbors of the site i). The off-diagonal elements H_{ij} randomly take values $\epsilon_{\mathrm{d}} > 0$ and $\epsilon_{\mathrm{m}} = (-1 + \mathrm{i}\kappa)\,|\epsilon'_{\mathrm{m}}|$, where the loss factor $\kappa = \epsilon''_{\mathrm{m}}/\,|\epsilon'_{\mathrm{m}}|$ is small in the optical and infrared spectral ranges, i.e., $\kappa \ll 1$. The diagonal elements H_{ii} are also random numbers distributed between $2d\epsilon_{\mathrm{m}}$ and $2d\epsilon_{\mathrm{d}}$, where $2d$ is the number of nearest neighbors in the lattice for a d-dimensional system.

It is important to note that the matrix $\widehat{\mathrm{H}}$ is similar to the quantum-mechanical Hamiltonian for Anderson's transition problem with both on- and off-diagonal correlated disorder [36,37]. We will refer hereafter to operator $\widehat{\mathrm{H}}$ as Kirchhoff's Hamiltonian (KH). In the approach considered here, the field distribution problem, i.e., the problem of finding a solution to the system of linear equations (2), can be translated into the problem of finding the eigenmodes of KH $\widehat{\mathrm{H}}$.

Suppose we have found the eigenvalues Λ_n for $\widehat{\mathrm{H}}$. In the optical and infrared spectral ranges, the real part ϵ'_{m} of the metal dielectric function ϵ_{m} is negative ($\epsilon'_{\mathrm{m}} < 0$), whereas the permittivity of a dielectric host is positive ($\epsilon_{\mathrm{d}} > 0$); as mentioned, the loss factor is small, $\kappa = \epsilon''_{\mathrm{m}}/|\epsilon'_{\mathrm{m}}| \ll 1$. Therefore, the manifold of the KH eigenvalues Λ_n contains the eigenvalues that have their real parts equal (or close) to zero with very small imaginary parts ($\kappa \ll 1$). Then the eigenstates that correspond to the eigenvalues $|\Lambda_n/\epsilon_{\mathrm{m}}| \ll 1$ are strongly excited by the external field and are seen as giant field fluctuations, representing nonuniform plasmon resonances of a percolation system.

The localized optical excitations can be thought of as field peaks separated, on average, by the distance $\xi_{\mathrm{e}} \propto a\,(N/n)^{1/d}$, where n is the number of the resonant KH eigenmodes excited by the external field and N is the total number of the eigenstates. In the limit $\kappa \ll 1$, only a small part $n \sim \kappa N$ of the eigenstates is effectively excited by the external field. Therefore, the distance ξ_{e}, which we call the field correlation length, is large: $\xi_{\mathrm{e}}/a \propto \kappa^{1/d} \gg 1$.

According to the one-parameter scaling theory, the eigenstates Ψ_n are, it is thought, all localized for the two-dimensional case (see, however, the discussion in [38,39]). On the other hand, it was shown that there is a transition from chaotic eigenstates [40,41] to the strongly localized eigenstates in the two-dimensional Anderson problem [42] with an intermediate crossover region. The KH also has strong off-diagonal disorder, $\langle \mathrm{H}'_{ij} \rangle = 0$ $(i \neq j)$, which usually favors localization [43,44]. Our conjecture is that the eigenstates Ψ_n are localized, at least those with $\Lambda_n \approx 0$, in a two-dimensional system. (We cannot, however, rule out the possibility of inhomogeneous localization similar to that obtained for fractals [45] or power-law localization [36,46].)

The Anderson transition in a three-dimensional system is less understood and little is known about the eigenfunctions [36,47]. We conjecture that the eigenstates with $\Lambda_n \approx 0$ are also localized in the three-dimensional case.

3 Scaling in Local-Field Distribution

For the films concerned, gaps between metal grains are filled by a dielectric substrate, so that a semicontinuous metal film can be thought of as a $2d$ array of metal and dielectric grains randomly distributed over the plane. The dielectric constant of a metal can be approximated by the Drude formula

$$\epsilon_{\mathrm{m}} = \epsilon_{\mathrm{b}} - (\omega_{\mathrm{p}}/\omega)^2/(1 + i\omega_\tau/\omega)\,, \tag{4}$$

where ϵ_{b} is the interband contribution, ω_{p} is the plasma frequency, and ω_τ is the plasmon relaxation rate ($\omega_\tau \ll \omega_{\mathrm{p}}$). In the high-frequency range considered here, losses in metal grains are relatively small, $\omega_\tau \ll \omega$. Therefore, the real part ϵ'_{m} of the metal dielectric function ϵ_{m} is much larger (in modulus) than the imaginary part ϵ''_{m}, i.e., the loss parameter κ is small, $\kappa = \epsilon''_{\mathrm{m}}/|\epsilon'_{\mathrm{m}}| \cong \omega_\tau/\omega \ll 1$. We note that ϵ'_{m} is negative for frequencies ω less than the renormalized plasma frequency,

$$\tilde{\omega}_{\mathrm{p}} = \omega_{\mathrm{p}}/\sqrt{\epsilon_{\mathrm{b}}}\,. \tag{5}$$

It is instructive to consider first the special case of $-\epsilon'_{\mathrm{m}} = \epsilon_{\mathrm{d}}$, where $\epsilon_{\mathrm{m}} \equiv \epsilon'_{\mathrm{m}} + i\epsilon''_{\mathrm{m}}$ and ϵ_{d} are the dielectric constants of the metallic and dielectric components, respectively. The condition $-\epsilon'_{\mathrm{m}} = \epsilon_{\mathrm{d}}$ corresponds to the resonance of individual metal particles in a dielectric host in the two-dimensional case. For simplicity, we also set $-\epsilon_{\mathrm{m}} = \epsilon_{\mathrm{d}} = 1$, which can always be done by simply renormalizing the corresponding quantities.

It can be shown that the field distribution on a percolation film at $-\epsilon_{\mathrm{m}} = \epsilon_{\mathrm{d}} = 1$ formally maps the Anderson metal–insulator transition problem [2,5,6]. In accord with this, the field potential representing the plasmon modes of a percolation film must be characterized by the same spatial distribution as the electron wave function in the Anderson transition problem. Such mathematical equivalence of the two physically different problems stems from the fact that the current conservation law for a percolation film acquires (when written in the discretized form) the form of Kirchhoff's equations, which, in turn, (when written in the matrix form) become identical to the equations describing the Anderson transition problem [6]. The corresponding Kirchhoff Hamiltonian for the field distribution problem is given by a matrix with random elements which can be expressed in terms of the dielectric constants for metal and dielectric bonds of the lattice representing the film. In this matrix, the values $\epsilon_{\mathrm{m}} = -1$ and $\epsilon_{\mathrm{d}} = 1$ appear in the matrix elements with probability p and $(1-p)$, respectively (where p is the metal filling factor given at percolation by $p = p_{\mathrm{c}}$, with $p_{\mathrm{c}} = 1/2$ for a self-dual system). In such a form, the Kirchhoff Hamiltonian is characterized by a random matrix, similar to that in the Anderson transition problem, with both on- and off-diagonal disorder. Based on this mathematical equivalence, it was concluded in [2,5,6] that the plasmons in a percolation film can experience Anderson-type localization within small areas, and the size is given by the Anderson length ξ_{A}. For most localized plasmon modes, ξ_{A} can be as small as one grain a.

Below, we develop a simple scaling approach that explains the nontrivial field distribution predicted and observed in percolation films. This scale-renormalization method supports the main conclusions of a rigorous (but tedious) theory of [2,5,6] and has the virtue of being simple and clear, which is important for understanding and interpreting future experiments.

First, we estimate the field in the hot spots for $-\epsilon'_{\mathrm{m}} = \epsilon_{\mathrm{d}}$. Hereafter, we use the sign * (not to be confused with complex conjugation) to indicate that the quantity concerned is given for $-\epsilon'_{\mathrm{m}} = \epsilon_{\mathrm{d}}$ (with $\epsilon_{\mathrm{d}} \sim 1$); for ξ_{A}, however, we omit this sign since this quantity always refers to $-\epsilon'_{\mathrm{m}} = \epsilon_{\mathrm{d}}$.

Since ϵ'_{m} is negative at optical frequencies, metal particles can be roughly thought of as inductor-resistor (L–R) elements, whereas the dielectric gaps between the particles can be treated as capacitive (C) elements. Then, the condition $\epsilon'_{\rm m} = -\epsilon_{\rm d}$ means that the conductivities of the L–R and C elements are equal in magnitude and opposite in sign, i.e., there is a resonance in the equivalent L–R–C circuit corresponding to individual particles.

The local field in resonating particles is enhanced by the resonance quality factor Q which is the inverse of the loss factor, $Q = \kappa^{-1}$, so that

$$E^*_{\rm m} \sim E_0 \kappa^{-1} (a/\xi_{\rm A})^d , \tag{6}$$

where the factor $(a/\xi_{\rm A})^2$ takes into account that the resonating mode is localized within $\xi_{\rm A}$. The resonant modes excited by a monochromatic light represent only the fraction κ of all modes so that the average distance (referred to as the field correlation length $\xi^*_{\rm e}$) between the field peaks is given by

$$\xi^*_{\rm e} \sim a/\kappa^{1/d} \gg \xi_{\rm A} . \tag{7}$$

Note that the field peaks associated with the resonance plasmon modes represent in fact the normal modes, with the near-zero eigennumbers, of Kirchhoff's Hamiltonian discussed above [2,6]. These modes are strongly excited by the applied field and seen as giant field fluctuations on the surface of the film.

Now we turn to the important case of "high contrast," with $|\epsilon_{\rm m}| \gg \epsilon_{\rm d}$, that corresponds to the long-wavelength part of the spectrum where the local-field enhancement can be especially strong. From the basic principles of Anderson localization [2], it is clear that a higher contrast favors localization, so that plasmon modes are expected to be localized in this case as well.

It is clear that at $|\epsilon_{\rm m}| \gg \epsilon_{\rm d}$, individual metal particles cannot resonate. We can renormalize, however, the high-contrast system to the case of $-\epsilon'_{\rm m} = \epsilon_{\rm d}$ considered above by formally "dividing" the film into square elements of the special resonant size

$$l_{\rm r} = a\Big(|\epsilon_{\rm m}|/\epsilon_{\rm d}\Big)^{\nu/(t+s)} \tag{8}$$

and considering these squares as new renormalized elements of the film. Really, using the known scaling dependences [1,4] for "metal" and "dielectric" squares of size l (which, respectively, do or do not contain a metal continuous path through the square):

$$\epsilon_{\rm m}(l) \sim (l/a)^{-t/\nu} \epsilon_{\rm m} \tag{9}$$

and

$$\epsilon_{\rm d}(l) \sim (l/a)^{s/\nu} \epsilon_{\rm d} , \tag{10}$$

we find that the dielectric constants of the renormalized elements with the size $l = l_{\rm r}$ are equal in magnitude and opposite in sign,

$$-\epsilon_{\rm m}(l_{\rm r}) = \epsilon_{\rm d}(l_{\rm r}) . \tag{11}$$

Thus, for these renormalized elements of size $l_{\rm r}$, there is a resonance similar to the resonance in the R–L–C circuit describing individual metal particles in a dielectric host. In this case, however, some effective (renormalized) R–L–C circuits represent resonating square elements.

For a two-dimensional percolation film, the critical exponents are given by $t \approx s \approx \nu \approx 4/3$; they represent the percolation critical exponents for conductivity, dielectric constant, and percolation correlation length, respectively [1,4]. Below, for simplicity we consider the two-dimensional case (d = 2), though all results can be easily generalized for arbitrary d.

In the renormalized system, the estimate obtained above for field peaks still holds. Since the electrical field and eigenfunction both scale as $l_{\rm r}$, we arrive at the conclusion that in the high-contrast system (with $|\epsilon_{\rm m}| \gg \epsilon_{\rm d}$), the field maxima can be estimated as

$$\begin{aligned} E_{\rm m} &\sim (l_{\rm r}/a)E^*_{\rm m} \sim E_0\kappa^{-1}(l_{\rm r}/a)(a/\xi_{\rm A})^2 \sim E_0\kappa^{-1}(l_{\rm r}/\xi_{\rm A})^2 \\ &\sim E_0(a/\xi_{\rm A})^2|\epsilon_{\rm m}|^{3/2} \Big/ \left(\epsilon_{\rm d}^{1/2}\epsilon''_{\rm m}\right) . \end{aligned} \tag{12}$$

The light-induced eigenmodes in the high-contrast system are separated, on average, by the distance $\xi_{\rm e}$ that exceeds the mode separation $\xi^*_{\rm e}$ at $\epsilon_{\rm m} = -\epsilon_{\rm d}$ by factor $l_{\rm r}/a$,

$$\xi_{\rm e} \sim (l_{\rm r}/a)\xi^*_{\rm e} \sim l_{\rm r}/\sqrt{\kappa} \sim a|\epsilon_{\rm m}|/\sqrt{\epsilon''_{\rm m}\epsilon_{\rm d}} . \tag{13}$$

For a Drude metal at $\omega \ll \omega_{\rm p}$, the local field peaks, according to (4) and (12), are given by

$$E_{\rm m}/E_0 \sim \epsilon_{\rm d}^{-1/2}(a/\xi_{\rm A})^2(\omega_{\rm p}/\omega_\tau) , \tag{14}$$

and the distance between the excited modes (13) is estimated as

$$\xi_{\rm e} \sim a\omega_{\rm p}/\sqrt{\epsilon_{\rm d}\omega\omega_\tau} . \tag{15}$$

Figure 1 illustrates, as described above, the renormalization of the field peaks and their spatial separations at the transition between the reference (renormalized) system with $-\epsilon_{\rm m} = \epsilon_{\rm d} = 1$ and the high-contrast system of $|\epsilon_{\rm m}/\epsilon_{\rm d}| \gg 1$.

As follows from the figure, the largest local fields of amplitude $E_{\rm m}$ result from excitation of the resonant clusters of size $l_{\rm r}$. At $-\epsilon_{\rm m} = \epsilon_{\rm d} = 1$, $l_{\rm r} = a$ (8), as in the reference system. With increasing wavelength (and thus the contrast $|\epsilon_{\rm m}|/\epsilon_{\rm d}$), the resonant size $l_{\rm r}$ and the distance $\xi_{\rm e}$ between the resonating modes both increase.

The above results have a clear physical interpretation and can also be obtained from the following complementary considerations. Let us consider two metal clusters, with conductance $\Sigma_{\rm m} = -{\rm i}(a/4\pi)\omega\epsilon_{\rm m}(l)$, separated by a dielectric gap, with conductance $\Sigma_{\rm d} = -{\rm i}(a/4\pi)\omega\epsilon_{\rm d}(l)$, as shown in Fig. 2a. The clusters and the gap are both of size l, and $\epsilon_{\rm m}(l)$ and $\epsilon_{\rm d}(l)$ are defined in (9) and (10), respectively. The equivalent conductance $\Sigma_{\rm e}$ for $\Sigma_{\rm m}$ and $\Sigma_{\rm d}$

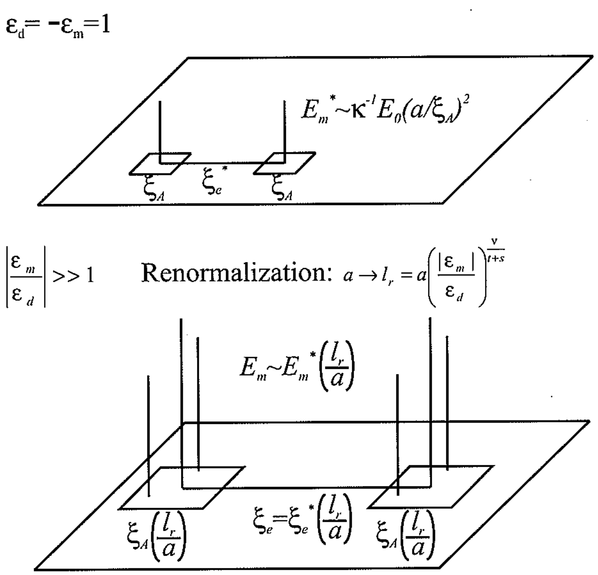

Fig. 1. Renormalization of the field distribution at the transition between the reference case with $-\epsilon_m/\epsilon_d = 1$ and the high-contrast case of $-\epsilon_m/\epsilon_d \gg 1$

in series is given by $\Sigma_e = \Sigma_m \Sigma_d \big/ (\Sigma_m + \Sigma_d)$, and the current j through the system is $j = \Sigma_e E_0 l$. The local field, however, is strongly inhomogeneous, and the largest field occurs at the point of the closest approach between the clusters, where the separation between clusters can be as small as a; then, the maximum field E_m is estimated as $E_m = (j/\Sigma_d)/a \sim E_0(l/a) \Big/ \left[1 + (l/a)^{(t+s)/\nu} \epsilon_d/\epsilon_m\right]$ [where we used (9) and (10)]. For the "resonant" size $l = l_r$, the real part of the denominator in the expression for E_m becomes zero, and the field E_m reaches its maximum, where it is estimated as $E_m/E_0 \sim \kappa^{-1}(l_r/a)$.

In the estimate obtained, we assumed, for simplicity, that $\xi_A \sim a$ and, in this limit, we reproduced the result (12). To obtain the "extra factor" $(a/\xi_A)^2$ of (12), we have to take into account that the localization area for the field is ξ_A rather than a, so that the field peak is "spread over" for the distance ξ_A. With this correction, we immediately arrive at formula (12).

It is clear that for any frequency of the applied field ω, there are always resonant clusters of the size (8)

$$l = l_r(\omega) \sim a(\omega/\tilde{\omega}_p)^{2\nu/(t+s)}, \tag{16}$$

where the local field reaches its maximum E_m. The resonant size l_r increases with the wavelength. It is important that at percolation, the system is scale-invariant so that all possible sizes needed for resonant excitation are present, as schematically illustrated in Fig. 1b. At some large wavelength, only large clusters of appropriate sizes resonate, leading to field peaks at the points of

closest approach between the metal clusters; with the decrease of the wavelength of the applied field, the smaller clusters begin to resonate, whereas the larger ones (as well as the smaller ones) are off the resonance, as shown in Fig. 1b.

We can also estimate the number $n(l_r)$ of field peaks within one resonating square of size l_r. In the high-contrast system (with $|\epsilon_m/\epsilon_d| \gg 1$), each field maximum of the renormalized system (with $|\epsilon_m/\epsilon_d| = 1$) splits into $n(l_r)$ peaks of E_m amplitude located along a dielectric gap in the "dielectric" square of size l_r (Figs. 1 and 2). The gap "area" scales as the capacitance of the dielectric gap, and so must the number of field peaks in the resonance square. Therefore, we estimate that

$$n(l_r) \propto (l_r/a)^{s/\nu_p}. \tag{17}$$

In accordance with the above considerations, the average (over the film surface) intensity of the local field is enhanced as

$$\left\langle \left|\frac{E}{E_0}\right|^2 \right\rangle \sim (E_m/E_0)^2 n(l_r)(\xi_A/\xi_e)^2 \sim (a/\xi_A)^2 |\epsilon_m|^{3/2} \big/ (\epsilon_m'' \epsilon_d), \tag{18}$$

where we used (8), (13), and (17) and the critical exponents $t = s = \nu = 4/3$.

In Fig. 3, we also show the simulated field distribution on a silver–glass percolation film at two different wavelengths. In accordance with the consideration above, we see that the local-field distribution consists of clusters of very sharp peaks where the spatial separation increases with the wavelength. A qualitatively similar field distribution was detected in recent experiments [5] using scanning near-field optical microscopy.

Thus, using simple arguments based on the scaling dependences of $\epsilon_m(l)$ and $\epsilon_d(l)$ on l and the resonance condition $-\epsilon_m(l_r) = \epsilon_d(l_r)$, one can define the renormalization procedure that allows one to rescale the "high-contrast" system to the renormalized one with $-\epsilon_m = \epsilon_d = 1$.

Below we show that the enhanced local field in the hot spots results in giant enhancement of *nonlinear* optical responses of semicontinuous films.

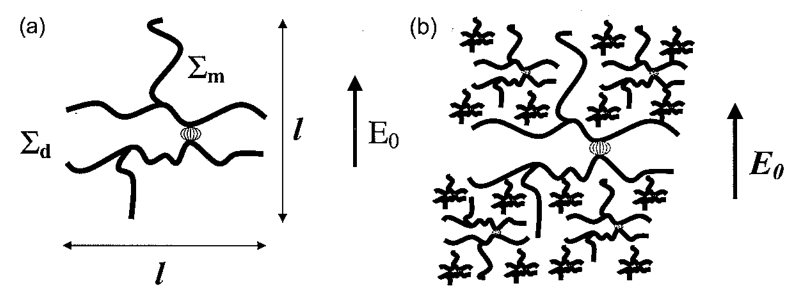

Fig. 2. **(a)** A typical element of a percolation film consisting of two conducting metal clusters with a dielectric gap in between. **(b)** Different resonating elements of a percolation film at different wavelengths

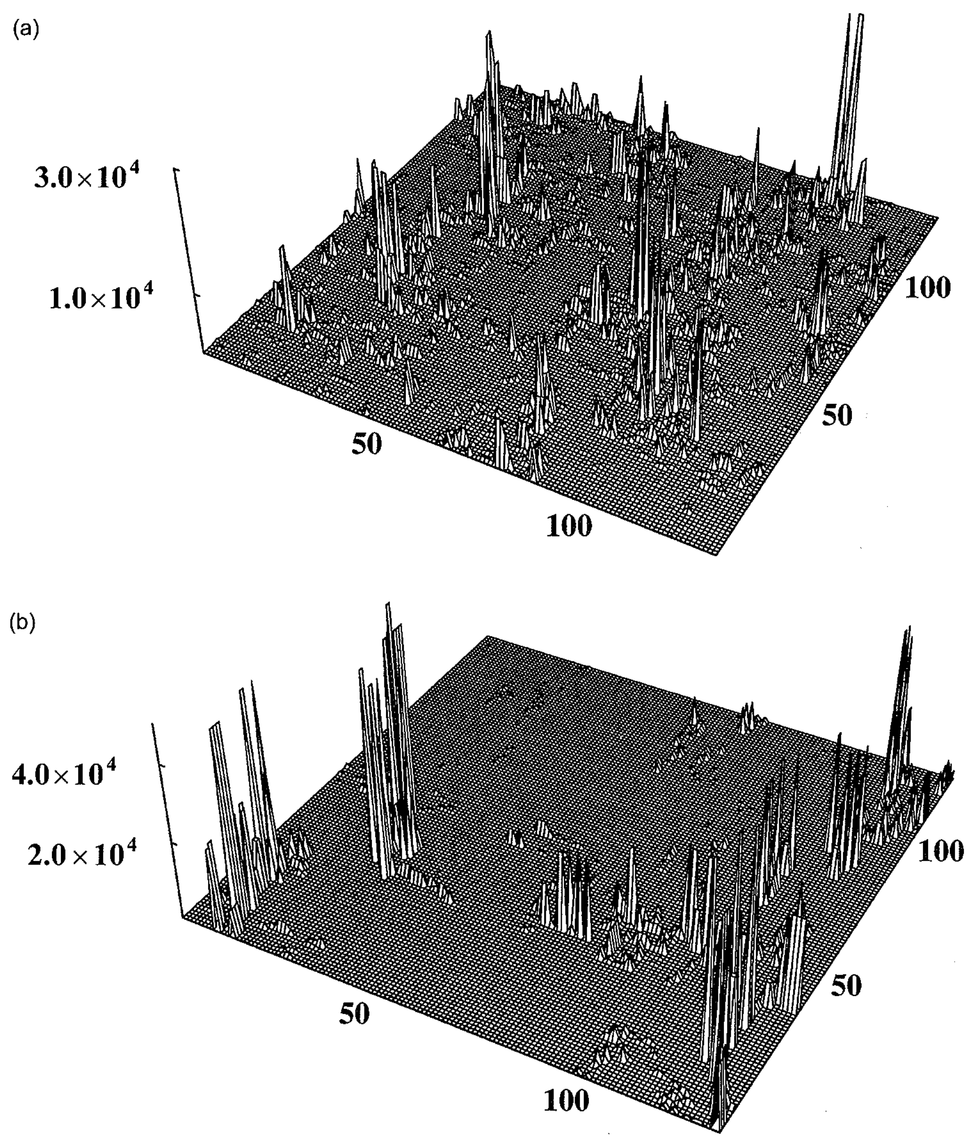

Fig. 3. Local-field distribution on a silver-glass percolation film at different wavelengths: **(a)** $\lambda = 1.5\,\mu\text{m}$ and **(b)** $\lambda = 10\,\mu\text{m}$

4 Enhanced Optical Nonlinearities

In general, we can define the high-order field moments as

$$M_{n,m} = \frac{1}{SE_0^m \left|E_0\right|^n} \int \left|E\left(\mathbf{r}\right)\right|^n E^m\left(\mathbf{r}\right)\, \mathrm{d}\mathbf{r}\,, \tag{19}$$

where, as above, E_0 is the amplitude of the external field and $E(\mathbf{r})$ is the local field [note that $E^2\left(\mathbf{r}\right) \equiv \mathbf{E}\left(\mathbf{r}\right) \cdot \mathbf{E}\left(\mathbf{r}\right)$]. The integration is over the entire surface S of the film.

The high-order field moment $M_{2k,m} \propto E^{k+m}E^{*k}$ represents a nonlinear optical process in which, in one elementary act, $k+m$ photons are added and k photons are subtracted [22] because the complex conjugated field in the general expression for nonlinear polarization implies photon subtraction, so that the corresponding frequency enters the nonlinear susceptibility with a minus sign [22]. As first shown in [6], enhancement is significantly different for nonlinear processes with photon subtraction in comparison with those where all photons enter the nonlinear susceptibility with a plus sign. The enhancement of Kerr optical nonlinearity G_K (see below) is equal to $M_{2,2}$, second-harmonic generation (SHG) and third-harmonic generation (THG) enhancements are given by $|M_{0,2}|^2$ and $|M_{0,3}|^2$, respectively, and surface-enhanced Raman scattering (SERS) is represented by $M_{4,0}$.

The high-order moments of the local field in $d = 2$ percolation films can be estimated as $M_{n,m} \sim (E_\mathrm{m}/E_0)^{n+m} n(l_\mathrm{r})(\xi_\mathrm{A}/\xi_\mathrm{e})^2$. Using the scaling formulas (8)–(17) for the field distribution, we obtain the following estimate for the field moments:

$$M_{n,m} \sim \left(\frac{E_\mathrm{m}}{E_0}\right)^{n+m} \frac{(l_\mathrm{r}/a)^{s/\nu}}{(\xi_\mathrm{e}/\xi_\mathrm{A})^2} \sim \left(\frac{|\epsilon_\mathrm{m}|^{3/2}}{(\xi_\mathrm{A}/a)^2 \epsilon_\mathrm{d}^{1/2} \epsilon''_\mathrm{m}}\right)^{n+m-1}, \tag{20}$$

for $n+m > 1$ and $n > 0$ (where we took into account that for two-dimensional percolation composites, the critical exponents are given by $t \cong s \cong \nu \cong 4/3$).

Since $|\epsilon_\mathrm{m}| \gg \epsilon_\mathrm{d}$ and the ratio $|\epsilon_\mathrm{m}|/\epsilon''_\mathrm{m} \gg 1$, the moments of the local field are very large, i.e., $M_{n,m} \gg 1$, in the visible and infrared spectral ranges. Note that the first moment, $M_{0,1} \simeq 1$, corresponds to the equation $\langle \mathbf{E}\left(\mathbf{r}\right)\rangle = \mathbf{E}_0$.

Now consider the moments $M_{n,m}$ for $n = 0$, i.e., $M_{0,m} = \left\langle E^m\left(\mathbf{r}\right)\right\rangle / \left(E_0\right)^m$. In the renormalized system where $\epsilon_\mathrm{m}(l_\mathrm{r})/\epsilon_\mathrm{d}(l_\mathrm{r}) \cong -1 + i\kappa$, the field distribution coincides with the field distribution in the system with $\epsilon_\mathrm{d} \simeq -\epsilon'_\mathrm{m} \sim 1$. In that system, field peaks E^*_m, differ in phase and cancel each other out, resulting in the moment $M^*_{0,m} \sim O\left(1\right)$ [6]. In transition to the original system, the peaks increase by the factor l_r, leading to an increase in the moment $M_{0,m}$. Then, using (8), (13), and (17), we obtain the following equation for the moment:

$$M_{0,m} \sim M^*_{0,m}(l_\mathrm{r}/a)^m \left[\frac{n(l_\mathrm{r})}{\left(\xi_\mathrm{e}/a\right)^2}\right] \sim \kappa(l_\mathrm{r}/a)^{m-2+s/\nu} \sim \frac{\epsilon''_\mathrm{m}|\epsilon_\mathrm{m}|^{(m-3)/2}}{\epsilon_\mathrm{d}^{(m-1)/2}}, \tag{21}$$

for $m > 1$ (where again we used the critical exponents $t \cong s \cong \nu \cong 4/3$).

For a Drude metal (4) and $\omega \ll \omega_p$, from (20) and (21), we obtain

$$M_{n,m} \sim \epsilon_d^{(1-n-m)/2} (a/\xi_A)^{2(n+m-1)} (\omega_p/\omega_\tau)^{n+m-1} , \quad (22)$$

for $n + m > 1$ and $n > 0$, and

$$M_{0,m} \sim \epsilon_d^{(1-m)/2} \left(\frac{\omega_p^{m-1} \omega_\tau}{\omega^m} \right) , \quad (23)$$

for $m > 1$.

Note that for all moments, the maximum in (22) and (23) is approximately the same (if $\xi_A \sim a$), so that

$$M_{n,m}^{(\max)} \sim \epsilon_d^{(1-n-m)/2} \left(\frac{\omega_p}{\omega_\tau} \right)^{n+m-1} . \quad (24)$$

However, in the spectral range $\omega_p \gg \omega \gg \omega_\tau$, moments $M_{0,m}$ gradually increase with wavelength, and the maximum is reached only at $\omega \sim \omega_\tau$, whereas the moments $M_{n,m}$ (with $n > 1$) reach this maximum at much shorter wavelengths (roughly, at $\omega \approx \tilde{\omega}_p/2$) and remain almost constant in the indicated spectral interval. This conclusion is supported by the numerical simulations for the silver–glass percolation films shown in Fig. 4; one can see that the above scaling formulas are in good accord with the simulations.

For silver–glass percolation films, with $\omega_p = 9.1$ eV and $\omega_\tau = 0.021$ eV, we find that the average field enhancement can be as large as $G_{RS} \sim M_{4,0} \sim 10^7$ for Raman scattering (see also Fig. 4), and as large as $G_{FWM} \sim |M_{2,2}|^2 \sim 10^{14}$ for degenerate four-wave mixing. According to Fig. 3, the local-field intensity in the hot spots can approach the magnitude 10^5 so that the local enhancement of nonlinear optical responses can be truly gigantic, up to 10^{10}, for Raman scattering, and up to 10^{20}, for four-wave mixing signals. With this level

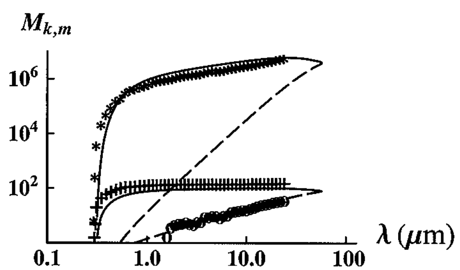

Fig. 4. Average enhancement of the high-order field moments $M_{n,m}$ in a percolation silver-glass two-dimensional film as a function of wavelength: $M_{4,0}$ [scaling formula (20) – *upper solid line* and numerical simulations – *]; $M_{0,4}$ [scaling formula (21) – *upper dashed line*]; $M_{2,0}$ [scaling formula (20) – *lower solid line* and numerical simulations – $^+$]; $M_{0,2}$ [scaling formula (21) – *lower dashed line* and numerical simulations – ^{0}]

of enhancement, one can perform *nonlinear* spectroscopy of single molecules and nanocrystals. It is important that the enhancement be obtained in the huge spectral range, from the near-UV to the far-infrared, which is a major virtue for spectroscopic studies of different molecules and nanocrystals. We also note that the field enhancement provided by semicontinuous metal films can be used for various photobiological and photochemical processes.

Acknowledgments

This work was supported in part by National Science Foundation under Grant DMR-0121 814, Petroleum Research Fund, Army Research Office under Grant DAAD19-01-1-0682, and NASA under Grants NAG 8-1710 and NCC-1-01049.

References

1. D. J. Bergman, D. Stroud, Solid State Phys. **46**, 147 (1992)
2. V. M. Shalaev, *Nonlinear Optics Of Random Media: Fractal Composites and Metal-Dielectric Films* (Springer, Berlin Heidelberg 2000)
3. A. K. Sarychev, V. M. Shalaev, Phys. Rep. **335**, 275 (2000)
4. D. Stauffer, A. Aharony, *Introduction to Percolation Theory*, 2 ed. (Taylor Francis, Philadelphia 1991)
5. S. Grésillon, L. Aigouy, A. C. Boccara, J. C. Rivoal, X. Quelin, C. Desmarest, P. Gadenne, V. A. Shubin, A. K. Sarychev, V. M. Shalaev, Phys. Rev. Lett. **82**, 4520 (1999)
6. A. K. Sarychev, V. A. Shubin, V. M. Shalaev, Phys. Rev. B **60**, 16389 (1999); A. K. Sarychev, V. M. Shalaev, Physica A **266**, 115 (1999); A. K. Sarychev, V. A. Shubin, V. M. Shalaev, Phys. Rev. E **59**, 7239 (1999)
7. H. J. Herrmann, S. Roux (Eds.) *Statistical Models for the Fracture of Disordered Media* (Elsevier North-Holland, Amsterdam 1990) and references therein
8. A. Aharony, Phys. Rev. Lett. **58**, 2726 (1987)
9. D. Stroud, P. M. Hui, Phys. Rev. B **37**, 8719 (1988)
10. V. M. Shalaev, M. I. Stockman, Sov. Phys. JETP **65**, 287 (1987); A. V. Butenko, V. M. Shalaev, M. I. Shtockman, Sov. Phys. JETP **67**, 60 (1988)
11. A. P. Vinogradov, A. V. Goldenshtein, A. K. Sarychev, Zh. Tekh. Fiz. **59**, 208 (1989) Engl. trans. in Sov. Phys. Techn. Phys. **34**, 125 (1989); V. A. Garanov, A. A. Kalachev, A. M. Karimov, A. N. Lagarkov, S. M. Matytsin, A. B. Pakhomov, B. P. Peregood, A. K. Sarychev, A. P. Vinogradov, A. M. Virnic, J. Phys. **3**, 3367 (1991); V. A. Garanov, A. A. Kalachev, S. M. Matytsin, I. I. Oblakova, A. B. Pakhomov, A. K. Sarychev, Zh. Tekh. Fiz. **62**, 44 (1992) [Engl. trans. Sov. Phys. Techn. Phys. (1992)]
12. D. J. Bergman, Phys. Rev. B **39**, 4598 (1989)
13. P. M. Hui, in *Nonlinearity and Breakdown in Soft Condensed Matter*, K. K. Bardhan, B. K. Chakrabarty, A. Hansen (Eds.), Lecture Notes Phys. **437** (Springer, Berlin, Heidelberg 1996)
14. V. M. Shalaev, Phys. Rep. **272**, 61 (1996)
15. V. M. Shalaev, A. K. Sarychev, Phys. Rev. B **57**, 13265 (1998)

16. Hongru Ma, Rongfu Xiao, Ping Sheng, J. Opt. Soc. Am. B **15**, 1022 (1998)
17. D. Stroud, Superlattice Microstruct. **23**, 567 (1998)
18. D. Bergman, O. Levy, D. Stroud, Phys. Rev. B **49**, 129 (1994); O. Levy, D. Bergman, Physica A **207**, 157 (1994); O. Levy, D. J. Bergman, D. G. Stroud, Phys. Rev. E **52**, 3184 (1995)
19. R. W. Cohen, G. D. Cody, M. D. Coutts, B. Abeles, Phys. Rev. B **8**, 3689 (1973)
20. J. P. Clerc, G. Giraud, J. M. Luck, Adv. Phys. **39**, 191 (1990)
21. C. Flytzanis, Prog. Opt. **29**, 2539 (1992) and references therein
22. R. W. Boyd, *Nonlinear Optics* (Academic, New York 1992); L. D. Landau, E. M. Lifshits, L. P. Pitaevskii, *Electromagnetics of Continuous Media*, 2nd ed. (Pergamon, Oxford 1984)
23. P. Sheng, *Introduction to Wave Scattering, Localization, and Mesoscopic Phenomena* (Academic, San Diego 1995)
24. D. A. G. Bruggeman, Ann. Phys. (Leipzig) **24**, 636 (1935)
25. X. C. Zeng, D. J. Bergman, P. M. Hui, D. Stroud, Phys. Rev. B **38**, 10970 (1988); X. C. Zeng, P. M. Hui, D. J. Bergman, D. Stroud, Physica A **157**, 10970 (1989)
26. D. J. Bergman, in *Composite Media and Homogenization Theory*, G. Dal Maso, G. F. Dell'Antinio (Eds.) (Birkhauser, Boston 1991) p. 67
27. O. Levy, D. J. Bergman, J. Phys. C **5**, 7095 (1993)
28. P. M. Hui, D. Stroud, Phys. Rev. B **49**, 11729 (1994)
29. H. C. Lee, K. P. Yuen, K. W. Yu, Phys. Rev. B **51**, 9317 (1995)
30. W. M. V. Wan, H. C. Lee, P. M. Hui, K. W. Yu, Phys. Rev. B **54**, 3946 (1996)
31. P. M. Hui, P. Cheung, Y. R. Kwong, Physica A **241**, 301 (1997) and references therein
32. F. Brouers et al., in *Fractals in the Natural and Applied Sciences* (Chapman Hall, London 1995) Chap. 24
33. F. Brouers, A. K. Sarychev, S. Blacher, O. Lothaire, Physica A **241**, 146 (1997)
34. F. Brouers, S. Blacher, A. N. Lagarkov, A. K. Sarychev, P. Gadenne, V. M. Shalaev, Phys. Rev. B **55**, 13234, (1997)
35. P. Gadenne, F. Brouers, V. M. Shalaev, A. K. Sarychev, J. Opt. Soc. Am. B **15**, 68 (1998)
36. B. Kramer, A. MacKinnon, Rep. Prog. Phys. **56**, 1469 (1993)
37. D. Belitz, T. R. Kirkpatrick, Rev. Mod. Phys. **66**, 261 (1994); M. V. Sadovskii, Phys. Rep. **282**, 225 (1997)
38. V. I. Fal'ko, K. B. Efetov, Phys. Rev. B **52**, 17413 (1995)
39. K. B. Efetov, *Supersymmetry in Disorder and Chaos* (Cambridge University Press, Cambridge 1997)
40. M. V. Berry, J. Phys. A **10**, 2083 (1977)
41. A. V. Andreev et al., Phys. Rev. Lett. **76**, 3947 (1996)
42. K. Muller et. al., Phys. Rev. Lett. **78**, 215 (1997)
43. J. A. Verges, Phys. Rev. B **57**, 870 (1998)
44. A. Elimes, R. A. Romer, M. Schreiber, Eur. Phys. J. B **1**, 29 (1998)
45. M. I. Stockman, Phys. Rev. E **56**, 6494 (1997); Phys. Rev. Lett. **79**, 4562 (1997); M. I. Stockman, L. N. Pandey, L. S. Muratov, T. F. George, Phys. Rev. B **51**, (1995); M. I. Stockman, L. N. Pandey, T. F. George, ibid. **53**, 2183 (1996)
46. M. Kaveh, N. F. Mott, J. Phys. A **14**, 259 (1981)
47. T. Kawarabayashi, B. Kramer, T. Ohtsuki, Phys. Rev. B **57**, 11842 (1998)

Surface-Plasmon-Enhanced Nonlinearities in Percolating 2-D Metal–Dielectric Films: Calculation of the Localized Giant Field and Their Observation in SNOM

Patrice Gadenne[1] and Jean C. Rivoal[2]

[1] Université de Versailles Saint Quentin, Laboratoire de Magnétisme et d'Optique, CNRS UMR 8624, F-78035 Versailles, France
gadenne@physique.uvsq.fr
[2] Université Pierre et Marie Curie, Laboratoire d'Optique Physique ESPCI, CNRS UPR 5, F-75231 Paris, France
rivoal@optique.espci.fr

Abstract. The surfaces of percolating random 2-D metal–dielectric films consist of several spectral resonances, which have been calculated and afterward observed by near-field optical microscopy. These films show anomalous optical properties which are investigated in the first section. Nonlinear electrical and optical properties of metal–dielectric film percolation composites, though recognized very early, were not well understood. It is only recently that calculation of local fields in semicontinuous films allows us to define the enhancement factors of optical nonlinearities. These calculations are outlined from basic principles in the second section and compared with experimental results. An insightful approach to the same problem is to use a network description to represent the random system and discretize the equations satisfied by the scalar potential of the electrical field. We recall in the third section how such discretization leads to a Hamiltonian which is paradigmatic in the theory of Anderson localization. The imaging and spectroscopy of localized optical excitation in gold-on-glass percolation films was performed using near-field optical microscopy (SNOM), and the fourth section recalls the basic features of the experimental technique and describes the first experimental observation of "hot spots" in a nanometer-scale area.

1 Introduction

In a significantly wide range close to the percolation second-order transition, granular metal thin films are known to manifest electromagnetic properties that are absent for both components: bulk metal and dielectric.

Two-dimensional metal–dielectric films consist of a planar distribution of nanometer-sized metal grains randomly distributed on the surface of an insulating substrate; each metallic grain has about the same height (thickness) above the substrate. If the edges do not dominate the shape of the grains, we can assume that the metallic grains are not too far from cylinders, and then the ratio between the metal covered surface and the total surface of the

V. M. Shalaev (Ed.): Optical Properties of Nanostructured Random Media, Topics Appl. Phys. **82**, 185–213 (2002)